

Risk-Aware Linear-Quadratic Regulation with Temporally Coupled States [★]

Chuanning Wei ^a, Kin Fung Li ^a, Dionysis Kalogerias ^b, Margaret P. Chapman^{*, a}

^aThe Edward S. Rogers Sr. Department of Electrical and Computer Engineering, University of Toronto, 10 King's College Road, Toronto, ON, M5S 3G4, Canada

^bDepartment of Electrical and Computer Engineering, Yale University, New Haven, CT, 06520, USA

Abstract

We formulate and solve a discrete-time linear-quadratic regulation (LQR) problem in a finite horizon that penalizes temporal variability and stochastic variability of the state trajectory. Our approach enables the user to strike a balance between regulating the state and reducing temporal variability, with explicit sensitivity to risk. We achieve this by extending a risk measure called predictive variance to a setting with temporally coupled states. Numerical examples demonstrate the effect of temporal coupling in both risk-aware and risk-neutral control settings. Particularly, we observe that explicitly penalizing temporal variability alone can also reduce stochastic variability.

Key words: Stochastic control; Risk-aware optimal control; Temporally coupled states; Linear systems.

1 Introduction

In state regulation of a control system, the behavior of the state trajectory can differ as a result of design choices. In particular, one may prefer trajectories that vary slowly over time, if abrupt changes in the state are undesirable. The design of slowly varying, continuous-time trajectories (small $|\dot{x}|$) has been studied in [13, 19, 20], among many others, whereas this brief paper concerns the design of slowly varying, discrete-time trajectories (small $|x_t - x_{t-1}|$). The goal to design slowly varying trajectories arises naturally in areas such as robotics and mechatronics [2, 15, 16], building climate control [30, 42], and even medicine [31]. For example, the path of a robot can be designed to be short by penalizing the distance between subsequent states [16, Eq. 8]. Additionally, in building climate control, occupants were found to prefer raising the temperatures of their air conditioners gradually rather than abruptly, which incentivizes energy sav-

ings [42]. Another example is that large glycemic variability, i.e., fluctuations in blood glucose level, is linked to diabetic complications [31]. Motivated by such examples and viewing real-world uncertainties from a probabilistic perspective, we study a stochastic controller synthesis problem that rewards slowly varying trajectories. The setting of interest concerns standard linear systems, but we evaluate their performance in a manner that deviates from a classical stochastic viewpoint.

Classical stochastic optimal control summarizes uncertain performance on average and thus is not designed to manage rare events [1, 29, 41, 45, 46]. For example, the linear-quadratic-Gaussian problem minimizes the expectation of the LQR cost $\mathcal{J} := x_N^\top Q x_N + \sum_{t=0}^{N-1} x_t^\top Q x_t + u_t^\top R u_t$ and so lacks explicit sensitivity to the stochastic variability of \mathcal{J} . This limitation motivates the use of more nuanced measures of stochastic system performance in controller design. Fortunately, *risk measures* quantify a probability distribution in various ways, e.g., the mean of the upper tail, the spread relative to some value, and the mean under distributional ambiguity, offering different representations of risk [1, 8, 11, 35, 40, 43, 46]. This brief paper uses a variance-like measure to quantify risk for a fully observable linear system with additive noise and hence highlights literature in similar settings. For information about other types of risk-aware control and related topics, please see [1, 8, 35, 40, 46].

Reducing stochastic variability in system performance can be dated back to the minimal cost variance

[★] This work was supported by the Edward S. Rogers Sr. Department of Electrical and Computer Engineering at the University of Toronto, and the Natural Sciences and Engineering Research Council of Canada (NSERC) Discovery Grants Program [RGPIN-2022-04140]. Cette recherche a été financée par le Conseil de recherches en sciences naturelles et en génie du Canada (CRSNG). This work was not presented at an IFAC meeting and was not published in any conference proceedings.

* Corresponding author: M.P. Chapman (email address: margaret.chapman[at]utoronto.ca).

Email addresses: chuanning.wei[at]mail.utoronto.ca (C. Wei), calvinkf.li[at]mail.utoronto.ca (K.F. Li), dionysis.kalogerias[at]yale.edu (D. Kalogerias).

(MCV) problem studied by Sain in 1966, which minimizes the variance of an LQR cost subject to an expected cost constraint [37]. Another classical example is the linear-exponential-quadratic-Gaussian (LEQG) problem [48]. This problem minimizes the objective $-2\theta^{-1} \log \mathbb{E}(\exp(-\theta \mathcal{J}/2))$ with a risk-aversion parameter $\theta < 0$, which approximates a mean-variance objective locally [48]. LEQG is closely related to other problems in control theory. There is a correspondence between LEQG and a mixed $\mathcal{H}_2/\mathcal{H}_\infty$ control problem [18, 49]. Also, both the MCV problem and the LEQG problem (under a series expansion of the LEQG objective) can be viewed as special cases of controlling the statistics of the distribution of an LQR cost [26, 38]. However, the Gaussian noise assumptions in [26, 48] imply that these controllers are not designed to handle more general noise distributions that may be skewed or heavy-tailed.

A modern approach for managing stochastic variability in linear system performance is to incorporate the *predictive variance* measure into an optimal control problem [44]. This measure assesses the variability of the state energy $x_t^\top Q x_t$ relative to the predicted average state energy at time t [44]. It takes the form of $\mathbb{E}((x_t^\top Q x_t - \mathbb{E}(x_t^\top Q x_t | h_{t-1}))^2)$, where h_{t-1} contains historical information before time t [44]. Predictive variance is an attractive risk measure for fully observable linear systems with additive noise for several reasons. First, the noise need not be Gaussian [44]. Second, an optimal controller that is affine state-feedback and depends on the skewness of the noise can be computed in closed-form via a Riccati recursion [44]. Third, predictive variance assesses risk in an interpretable way in terms of stochastic variability in a dynamic setting [44]. This type of risk assessment is a natural choice when variability above and below a benchmark (the predicted average state energy in this case) should be penalized evenly [41, 46]. Also, note that using variance as a measure of risk has a rich history in financial portfolio management; e.g., see [14]. The predictive variance approach has been extended to the infinite-horizon case [50], partially observable systems [43], interconnected systems [34, 47], and model predictive control [12], showing its applicability to various LQ control problems. In the current work, we connect predictive variance to the aim of rewarding state trajectories that vary gradually over time. To achieve this, first we extend both the state energy and the predictive variance to be defined for a portion of the state trajectory, where the involved states are said to be *temporally coupled*. Then, we propose and solve an optimal control problem where the risk measure is the predictive variance for temporally coupled states.¹ Though experimentation, we observe that a reduction in temporal variability can even induce a reduction in stochastic

¹ In contrast, one of the current authors studies a risk-aware control problem involving a different risk measure without temporal coupling and a class of nonlinear systems with multiplicative and additive noise in [33].

variability (i.e., risk aversion) when predictive variance is absent from the optimal control problem.

Temporal coupling reflects the behavior of a stochastic control system *over a time period* (of stages) rather than at a single stage. We refer to behavior over such a period as trajectory-wise behavior. Practical examples include the path length traversed by a robot [16], the maximum rate of power drawn from an electric grid [25], and a system's maximum distance outside a safe region [10]. In contrast, stage-wise behavior, like the robot's current location or the instantaneous rate of power, only indicate behavior briefly in time. Trajectory-wise behavior can be formally specified by a *non-Markovian* objective functional, where the cost incurred at some stage is a functional of states at different times [4].

Now, consider the problem of optimizing a non-Markovian objective for a control system at hand. While dynamic programming (DP) is a standard approach for deriving optimal controllers, the system model in its given form may not be conducive to a direct application of DP. However, it may be valid to apply DP by first suitably augmenting the state with additional information [25]. Deterministic and stochastic DP with state augmentation has been studied in [25], where the authors developed examples involving the optimization of a maximum cost. State augmentation is also useful for solving some risk-aware optimal control problems; examples include problems whose objectives are defined in terms of the conditional value-at-risk (CVaR) measure [6, 10] and expected utility measures [7].² Applying DP to an augmented system increases numerical complexity [25], and the user must decide whether such complexity is acceptable for a given application. While this brief paper does not specifically address the numerical complexity challenge, we use an augmented state with a flexible dimension $n_t \leq n(\mathbf{k} + 1)$, where n is the original state dimension but \mathbf{k} can be adjusted. Our solution is based on a Riccati recursion, and the dimension of the inverted matrix does not depend on \mathbf{k} .

Contribution. We formulate and solve a nonstandard stochastic LQR problem in a risk-aware manner, i.e., with explicit sensitivity to rarer outcomes in addition to what is expected. The problem deviates from a standard regulation problem in that it allows the user to encode a preference for slowly varying state trajectories along with state regulation, for example, by penalizing both $(x_t - x_{t-1})^\top Q (x_t - x_{t-1})$ and $x_t^\top Q x_t$. We generalize this penalty using a convex quadratic cost that contains historical states over a period, a cost called the *sequential state energy*, and those states are said to be

² The CVaR represents an expected value in a given fraction of the worst cases [40]. An expected utility generalizes the exponential utility [7].

temporally coupled. We quantify risk by extending predictive variance [43, 44], a measure of stochastic variability, to be defined for the sequential state energy. The extended predictive variance is a *trajectory-wise* risk concept instead of a stage-wise one. That is, in general, the risk over a period consisting of distinct stages is not immediately separable into the risks over these stages, and such a separation may even be impossible. Thus, our problem differs from risk-aware control problems that concern stage-wise risk concepts, such as those in [5, 17, 24, 33, 36, 39, 43–45]. Since the (extended) predictive variance is defined via conditional expectation, we derive an analytical expression for it. This expression also turns out to be convex quadratic in the temporally coupled states (Lemmas 1–2). This nontrivial discovery allows us to reformulate our nonstandard problem (Problem 1) into a form that enjoys a well-known solution. An optimal controller can be found analytically via a Riccati recursion and is affine in a recent state history (Theorem 1, Corollary 1). Numerical examples illustrate tradeoffs that can arise from different parameter choices, and demonstrate the effect of temporal coupling in both risk-aware and risk-neutral control settings.

Organization. Section 2 formulates the optimal control problem (Problem 1). Section 3 presents an analytical expression for the (extended) predictive variance, reformulating Problem 1 into a problem with a quadratic non-Markovian objective (Problem 2). Section 4 reformulates Problem 2 into a standard form (Problem 3) via a suitable state augmentation, leading to an optimal controller. Section 5 presents numerical examples, and Section 6 offers future directions inspired by this work.

Notation. $\mathbb{N} := \{1, 2, 3, \dots\}$. $\mathbb{R}^{n \times m}$ is the set of $n \times m$ real matrices. $0_{n \times m}$ is the $n \times m$ matrix of all zeros. I_n is the $n \times n$ identity matrix. \mathcal{S}_n (\mathcal{S}_n^+) is the set of $n \times n$ real symmetric positive semidefinite (definite) matrices. $(\cdot)^\top$ denotes the matrix transpose. \oplus denotes the matrix direct sum [22, Def. 0.9.2]. $|\cdot|$ denotes the Euclidean norm. $\mathbb{E}(\cdot)$ ($\text{var}(\cdot)$) denotes expectation (variance). $y \in \mathcal{L}^2(\mathcal{F})$ specifies that y is an \mathcal{F} -measurable random vector such that $\mathbb{E}(|y|^2) < \infty$. $\sigma(\cdot)$ denotes the σ -algebra generated by a random vector [3, Def. 6.4.1]. a.s. stands for almost surely. We fix a parameter \mathbf{k} throughout Sections 2–4 and often suppress it from our notation for brevity. $\lambda \in [0, \infty)$ and $R \in \mathcal{S}_m^+$ are parameters representing the importance of penalizing risk and control effort, respectively. The symbol \mathbf{u} is shorthand for (u_0, \dots, u_{N-1}) .

2 Problem Formulation

Consider a fully observable, stochastic linear system in discrete time

$$x_{t+1} = Ax_t + Bu_t + w_t, \quad t \in \{0, \dots, N-1\}, \quad (1)$$

where $N \in \mathbb{N}$ is the horizon length, $A \in \mathbb{R}^{n \times n}$ and $B \in \mathbb{R}^{n \times m}$ are deterministic matrices, x_t is a \mathbb{R}^n -valued random vector (state), u_t is a \mathbb{R}^m -valued random vector (control), and w_t is a \mathbb{R}^n -valued random vector (disturbance). All random vectors are defined on a probability space $(\Omega, \mathcal{G}, \mathbb{P})$, and x_0, w_0, \dots, w_{N-1} are independent [28, p. 18]. We assume that w_0, \dots, w_{N-1} are identically distributed without imposing a particular distribution, although we impose an integrability condition below. We define $\mathcal{F}_t := \sigma(h_t)$, where h_t is a random vector specified by $h_t := [x_0^\top, u_0^\top, \dots, x_{t-1}^\top, u_{t-1}^\top, x_t^\top]^\top$ if $t \in \{1, \dots, N\}$ and $h_0 := x_0$. We assume that the initial state is deterministic, i.e., $x_0 = \mathbf{x}_0$ a.s., where $\mathbf{x}_0 \in \mathbb{R}^n$ is arbitrary. We also impose the following conditions:

Assumption 1 For every $t \in \{0, \dots, N-1\}$, (A1) u_t is causal and square-integrable, i.e., $u_t \in \mathcal{L}^2(\mathcal{F}_t)$; and (A2) w_t satisfies $\mathbb{E}(|w_t|^4) < \infty$.

While the square-integrability of x_0 and all controls and disturbances ensures that each x_t is square-integrable due to (1), the stronger assumption (A2) enables the use of a risk measure called predictive variance [44].³ Under the same assumption, next we extend predictive variance to the setting of temporally coupled states.

2.1 Sequential State Energy and its Predictive Variance

As motivated in Section 1, we study an optimal control problem (to be defined in Section 2.2) that penalizes temporal variability and stochastic variability of the state trajectory. To quantify temporal variability, we extend the state energy $x_t^\top Q x_t$ as follows: Given a *coupling length* $\mathbf{k} \in \{0, \dots, N\}$, we define for each $t \in \{0, \dots, N\}$ the *sequential state energy*

$$z_t := \eta_t^\top Q_t \eta_t, \quad (2)$$

where $\eta_t := [x_t^\top \dots x_{t-\mathbf{k}_t}^\top]^\top$ is the *truncated state history* containing $n_t := n(\mathbf{k}_t + 1)$ elements with $\mathbf{k}_t := \min\{\mathbf{k}, t\}$, and Q_t is the first n_t rows and first n_t columns of the matrix $Q \in \mathcal{S}_{n(\mathbf{k}+1)}$ denoted by

$$Q := \begin{bmatrix} Q_{00} & \cdots & Q_{0\mathbf{k}} \\ \vdots & \ddots & \vdots \\ Q_{\mathbf{k}0} & \cdots & Q_{\mathbf{k}\mathbf{k}} \end{bmatrix}. \quad (3)$$

Since $Q \in \mathcal{S}_{n(\mathbf{k}+1)}$ by assumption, it follows that $Q_t \in \mathcal{S}_{n_t}$ and $Q_{ii} \in \mathcal{S}_n$ for each i [22, Observation 7.1.2]. η_t encodes the state trajectory in at most $\mathbf{k} + 1$ recent times; the states in η_t are said to be temporally coupled

³ Strictly speaking, a risk measure is a map from a space of random variables to the extended real line [40]. Although predictive variance is defined in terms of multiple random objects, we still call it a risk measure for simplicity.

(introduced previously). For example, given $Q, \bar{Q} \in \mathcal{S}_n$, we can express the one-step temporally coupled cost

$$x_t^\top Q x_t + (x_t - x_{t-1})^\top \bar{Q} (x_t - x_{t-1}) \quad (4)$$

in the form of (2) using $\eta_t = [x_t^\top \ x_{t-1}^\top]^\top$ and $\mathcal{Q}_t = Q \oplus 0_{n \times n} + [-I_n \ I_n]^\top \bar{Q} [-I_n \ I_n]$.

Next, we quantify risk in terms of the stochastic variability of the recent state trajectory. We define the *predictive variance of the sequential state energy* by $\mathbb{E}(\Delta_t^2)$, where $\Delta_t := z_t - \mathbb{E}(z_t | \mathcal{F}_{t-1})$, for every $t \in \{1, \dots, N\}$. If $\mathbf{k} = 0$ and $Q_{00} = Q$, then the sequential state energy z_t (2) reduces to the state energy $x_t^\top Q x_t$, so that $\Delta_t = x_t^\top Q x_t - \mathbb{E}(x_t^\top Q x_t | \mathcal{F}_{t-1})$ and our definition of predictive variance coincides with the one defined for state energy in [44, Eq. 3]. Our construction enables the user to strike a balance between regulating the state and reducing temporal variability by permitting a cost function like (4).

2.2 Risk-Aware Optimal Control Problem

Using the predictive variance $\mathbb{E}(\Delta_t^2)$ defined in Section 2.1, we present the following optimal control problem:

Problem 1 *Under Assumption (A2), consider*

$$\begin{aligned} \inf_{\mathbf{u}} \quad & \mathcal{J}_\lambda(\mathbf{u}) \\ \text{subject to} \quad & \text{dynamics (1), } x_0 = \mathbf{x}_0 \text{ a.s.,} \\ & u_t \in \mathcal{L}^2(\mathcal{F}_t), t \in \{0, \dots, N-1\}, \end{aligned}$$

where the objective $\mathcal{J}_\lambda(\mathbf{u})$ is defined by

$$\mathcal{J}_\lambda(\mathbf{u}) := \mathbb{E} \left(z_N + \sum_{t=0}^{N-1} z_t + u_t^\top R u_t \right) + \lambda \mathbb{E} \left(\sum_{t=1}^N \Delta_t^2 \right). \quad (5)$$

Problem 1 allows the user to trade off various preferences related to λ , \mathcal{Q}_t , and \mathbf{k} . λ represents the relative importance of penalizing z_t (2) and control effort on average versus the stochastic variability of z_t . Hence, Problem 1 resembles a *mean-risk* optimization problem, which gives the user flexibility to make a compromise between reducing a cost on average versus reducing its uncertainty [40, Sec. 6.2]. \mathcal{Q}_t and \mathbf{k} offer finer control over the state trajectory, in addition to the typical goal of state regulation. z_t (2) expands to

$$z_t = \sum_{i=1}^{\mathbf{k}_t} \sum_{j=1}^{\mathbf{k}_t} x_{t-i}^\top Q_{ij} x_{t-j} + 2 \sum_{i=1}^{\mathbf{k}_t} x_{t-i}^\top Q_{i0} x_t + x_t^\top Q_{00} x_t, \quad (6)$$

where each term is bilinear in two states at possibly different times. x_t is coupled with a previous state x_{t-i} via $x_{t-i}^\top Q_{i0} x_t$, but only $x_t^\top Q_{00} x_t$ would take effect at time t in standard state regulation. In the special case

of (4), as \bar{Q} dominates Q , reducing the one-step state difference is preferred over driving the state to the origin. Previewing the experiments in Section 5, we find that small stochastic variability can arise not only in a setting with $\lambda > 0$, but also in a setting with large \mathbf{k} and $\lambda = 0$. The latter illustrates a link between temporal coupling and risk reduction, although risk is not explicit in \mathcal{J}_λ in this case.

Returning to the general form of Problem 1, we further describe its relation to the risk-aware control literature. Problem 1 explicitly quantifies risk in terms of stochastic variability while accounting for temporal variability, differing from many approaches. For example, approaches based on CVaR are designed to be sensitive to the (one-sided) tail but not the rest of a probability distribution [1, 9, 10, 27, 39, 45]. In contrast, variance-like measures, particularly our (extended) predictive variance, consider both sides of a distribution and quantify stochastic (two-sided) variability. This also differs from a nested risk representation [5, 36], which takes the form of $\rho_0(y_0 + \rho_1(y_1 + \dots))$ with y_t a random variable and ρ_t a map assessing risk at time t , where the nested structure can be difficult to interpret [23, 46]. It is pertinent to assess the risk of a control system in an interpretable way, especially when the system represents a real-world process [9, 29]. As well as being interpretable, Problem 1 involves a trajectory-wise risk assessment, thereby differing from [5, 17, 24, 33, 36, 39, 43–45], mentioned in Section 1. More specifically, Problem 1 penalizes the mean and risk of z_t (2), whose form enables the generation of slowly varying trajectories, to be illustrated in Section 5. Additionally, it will become clear that Problem 1 enjoys an analytical solution due to the linear dynamics and choice of objective functional (Section 4). Interpretable, trajectory-wise risk assessments were developed using CVaR [6, 9, 10] and expected utility measures [7] for Markov decision processes but do not admit analytical solutions in general. Having motivated Problem 1, we turn our attention to solving it through reformulation.

3 Reformulation to a Quadratic Form

To reformulate Problem 1, first we show that its objective enjoys a quadratic representation in appropriate variables in three steps. First, we decompose Δ_t^2 into a sum of three integrable terms and evaluate their expectations (Lemma 1). Then, we show that the predictive variance $\mathbb{E}(\Delta_t^2)$ is convex and quadratic in η_t (Lemma 2). Finally, we reformulate the objective $\mathcal{J}_\lambda(\mathbf{u})$ as a sum of convex quadratic functions in η_t and u_t (Lemma 3). These results are expressed in terms of the following stationary statistics, which are finite under Assumption 1: $\bar{w} := \mathbb{E}(w_{t-1})$, $\Sigma := \mathbb{E}(d_t d_t^\top)$, $\gamma := \mathbb{E}(d_t d_t^\top Q_{00} d_t)$, and $\delta := \text{var}(d_t^\top Q_{00} d_t)$, where $d_t := w_{t-1} - \bar{w}$ for every $t \in \{1, \dots, N\}$ [44]. The results are grounded in elementary measure and probability theory [3].

Lemma 1 *Let Assumption 1 hold and $t \in \{1, \dots, N\}$ be given. Define the prediction error of the state energy by $y_t := x_t^\top Q_{00} x_t - \mathbb{E}(x_t^\top Q_{00} x_t | \mathcal{F}_{t-1})$. Also, define*

$$\Delta_{t,1} := y_t^2, \quad (7a)$$

$$\Delta_{t,2} := 4 \left(\sum_{i=1}^{\mathbf{k}_t} x_{t-i}^\top Q_{i0} d_t \right)^2 \quad \text{if } \mathbf{k}_t \geq 1, \text{ and} \quad (7b)$$

$$\Delta_{t,3} := 4 \sum_{i=1}^{\mathbf{k}_t} x_{t-i}^\top Q_{i0} d_t y_t \quad \text{if } \mathbf{k}_t \geq 1. \quad (7c)$$

If $\mathbf{k}_t \geq 1$, then

$$\Delta_t^2 = \Delta_{t,1} + \Delta_{t,2} + \Delta_{t,3} \quad \text{a.s.}, \quad (8a)$$

where each term on the right-hand side is integrable,

$$\mathbb{E}(\Delta_{t,1}) = 4\mathbb{E}(x_t^\top Q_{00} \Sigma Q_{00} x_t + x_t^\top Q_{00} \gamma) + \vartheta, \quad (8b)$$

$$\mathbb{E}(\Delta_{t,2}) = 4 \sum_{i=1}^{\mathbf{k}_t} \sum_{j=1}^{\mathbf{k}_t} \mathbb{E}(x_{t-i}^\top Q_{i0} \Sigma Q_{0j} x_{t-j}), \quad (8c)$$

$$\mathbb{E}(\Delta_{t,3}) = 4 \sum_{i=1}^{\mathbf{k}_t} \mathbb{E}(x_{t-i}^\top Q_{i0} (\gamma + 2\Sigma Q_{00} x_t)), \quad (8d)$$

and $\vartheta := \delta - 4\text{tr}((\Sigma Q_{00})^2)$. If $\mathbf{k}_t = 0$, then $\Delta_t^2 = \Delta_{t,1}$ is integrable and $\mathbb{E}(\Delta_t^2)$ is given by (8b).

The proof of Lemma 1 is based on measure-theoretic principles and is presented in Appendix A. The special case of $\mathbf{k}_t = 0$ was derived in [44, Appendix] and is stated for completeness, while the terms $\Delta_{t,2}$ (7b) and $\Delta_{t,3}$ (7c) arise due to the temporally coupled states. Since x_{t-i} is \mathcal{F}_{t-1} -measurable for $i \in \{1, \dots, \mathbf{k}_t\}$, the submatrices Q_{ij} for i and j in $\{1, \dots, \mathbf{k}_t\}$ are absent from (7). However, these submatrices still appear in z_t in general. The above results can be expressed compactly. First, for each $t \in \{0, \dots, N\}$, we define $\zeta_t := 4[Q_{00}^\top \cdots Q_{\mathbf{k}_t 0}^\top]^\top \gamma$ and

$$H_t := 4 \begin{bmatrix} Q_{00} \Sigma Q_{00} & \cdots & Q_{00} \Sigma Q_{0\mathbf{k}_t} \\ \vdots & \ddots & \vdots \\ Q_{\mathbf{k}_t 0} \Sigma Q_{00} & \cdots & Q_{\mathbf{k}_t 0} \Sigma Q_{0\mathbf{k}_t} \end{bmatrix}.$$

Lemma 2 *Under Assumption 1, for any $t \in \{1, \dots, N\}$, we have $H_t \in \mathcal{S}_{n_t}$ and $\mathbb{E}(\Delta_t^2) = \mathbb{E}(\eta_t^\top H_t \eta_t + \zeta_t^\top \eta_t) + \vartheta$.*

Proof. To confirm that $H_t \in \mathcal{S}_{n_t}$, apply the decomposition $H_t = 4\bar{Q}_t^\top \Sigma \bar{Q}_t$, where $\bar{Q}_t := [Q_{00} \cdots Q_{0\mathbf{k}_t}]$ and $\Sigma \in \mathcal{S}_n$. The quadratic form of $\mathbb{E}(\Delta_t^2)$ follows from Lemma 1 and the additivity of expectations of integrable random variables [3, Th. 1.6.3]. \square

Lemma 3 *Under Assumption 1, $\mathcal{J}_\lambda(\mathbf{u})$ (5) satisfies*

$$\mathcal{J}_\lambda(\mathbf{u}) = \mathbb{E} \left(c_N(\eta_N) + \sum_{t=0}^{N-1} c_t(\eta_t, u_t) \right) + c, \quad (9)$$

where $c_N : \mathbb{R}^{n_N} \rightarrow \mathbb{R}$ and $c_t : \mathbb{R}^{n_t} \times \mathbb{R}^m \rightarrow \mathbb{R}$ are quadratic, λ -parameterized functions defined by

$$\begin{aligned} c_N(\eta) &:= \eta^\top Q_{\lambda, N} \eta + \lambda \zeta_N^\top \eta \quad \text{and} \\ c_t(\eta, u) &:= \eta^\top Q_{\lambda, t} \eta + \lambda \zeta_t^\top \eta + u^\top R u, \end{aligned} \quad (10)$$

respectively, $Q_{\lambda, t} := Q_t + \lambda H_t \in \mathcal{S}_{n_t}$ is the inflated state history penalty matrix for each $t \in \{0, \dots, N\}$, and $c := \lambda(N\vartheta - 4\mathbf{x}_0^\top Q_{00} \Sigma Q_{00} \mathbf{x}_0 - 4\gamma^\top Q_{00} \mathbf{x}_0)$ is a real number.

Proof. Apply Lemma 2 to the definition of $\mathcal{J}_\lambda(\mathbf{u})$ (5), particularly using the fact that η_0, \dots, η_N are square-integrable random vectors under Assumption 1. \square

Substituting (9) into Problem 1 yields the following problem (where we omit the constant term c):

Problem 2 *Under Assumption (A2), consider the optimal control problem (each c_t is defined in (10)):*

$$\begin{aligned} \mathcal{J}_\lambda^*(\mathbf{x}_0) &:= \inf_{\mathbf{u}} \quad \mathbb{E} \left(c_N(\eta_N) + \sum_{t=0}^{N-1} c_t(\eta_t, u_t) \right) \\ &\text{subject to} \quad \text{dynamics (1), } x_0 = \mathbf{x}_0 \text{ a.s.,} \\ &\quad u_t \in \mathcal{L}^2(\mathcal{F}_t), t \in \{0, \dots, N-1\}. \end{aligned}$$

Observe that the objectives of Problems 1 and 2 merely differ by a constant, and the constraints of these problems are identical. Thus, if \mathbf{u}^* is optimal for Problem 1, then \mathbf{u}^* is optimal for Problem 2, and vice versa. The objective of Problem 2 enjoys a particularly convenient form, being a sum of convex quadratic costs in η_t and u_t . This is useful for deriving an analytical expression for an optimal controller, to be presented next.

4 Risk-Aware Optimal Controller Synthesis

Here, we show that an optimal controller can be computed via a Riccati recursion and only requires the truncated state history η_t instead of the full history h_t . This is achieved by reformulating the system dynamics and the control constraints, using η_t as an augmented state.

Despite the dynamics (1) being Markovian (in the original state x_t), dynamic programming cannot be applied directly to Problem 2 in its current form because c_t is a function of η_t rather than x_t alone. To circumvent this issue, we express the dynamics (1) in terms of η_t , regarding η_t as a \mathbb{R}^{n_t} -valued random augmented state vector. For every $t \in \{0, \dots, N-1\}$, we define

$$\begin{aligned} A_t &:= \begin{cases} [A \ 0_{n \times n_{\mathbf{k}_t}}] & \text{if } \mathbf{k}_t \geq 1, \\ A & \text{if } \mathbf{k}_t = 0, \end{cases} \quad \text{for } \mathbf{k} \in \{0, \dots, N\}, \\ D_t &:= \begin{cases} [I_{n_{\mathbf{k}}} \ 0_{n_{\mathbf{k}} \times n}] & \text{if } t \geq \mathbf{k}, \\ I_{n_{(t+1)}} & \text{if } t < \mathbf{k}, \end{cases} \quad \text{for } \mathbf{k} \in \{1, \dots, N\}. \end{aligned}$$

Observe that A_t satisfies the relation $A_t \eta_t = A x_t$, and if $t \geq \mathbf{k}$, then $D_t \eta_t$ equals η_t without the earliest state $x_{t-\mathbf{k}}$. Then, the augmented dynamics are

$$\eta_{t+1} = f_t(\eta_t, u_t, w_t), \quad t \in \{0, \dots, N-1\}, \quad (11)$$

where we define $f_t : \mathbb{R}^{n_t} \times \mathbb{R}^m \times \mathbb{R}^n \rightarrow \mathbb{R}^{n_{t+1}}$ by $f_t(\eta, u, w) := \tilde{A}_t \eta + \tilde{B}_t u + \tilde{C}_t w$ and the matrices by

$$\tilde{A}_t := \begin{bmatrix} A_t \\ D_t \end{bmatrix}, \tilde{B}_t := \begin{bmatrix} B \\ 0_{n_{\mathbf{k}t+1} \times m} \end{bmatrix}, \tilde{C}_t := \begin{bmatrix} I_n \\ 0_{n_{\mathbf{k}t+1} \times n} \end{bmatrix}$$

if $\mathbf{k} \in \{1, \dots, N\}$, whereas $\tilde{A}_t := A$, $\tilde{B}_t := B$, and $\tilde{C}_t := I_n$ if $\mathbf{k} = 0$. The augmented dynamics (11) are Markovian (in η_t) and linear. However, unlike a standard LQR set-up, the state space \mathbb{R}^{n_t} of (11) is time-varying. For convenience, we define $\mathcal{G}_t := \sigma(g_t)$ with $g_t := [\eta_0^\top, u_0^\top, \dots, \eta_{t-1}^\top, u_{t-1}^\top, \eta_t^\top]^\top$ if $t \in \{1, \dots, N\}$ and $g_0 := \eta_0$, analogous to the definitions of \mathcal{F}_t and h_t , respectively. As a final step in the reformulation, we pose the following problem and show its connection to Problems 1–2 (see Theorem 1):

Problem 3 *Under Assumption (A2), consider the optimal control problem (each c_t is defined in (10)):*

$$\begin{aligned} \inf_{\mathbf{u}} \quad & \mathbb{E} \left(c_N(\eta_N) + \sum_{t=0}^{N-1} c_t(\eta_t, u_t) \right) \\ \text{subject to} \quad & \text{dynamics (11), } \eta_0 = \mathbf{x}_0 \text{ a.s.,} \\ & u_t \in \mathcal{L}^2(\mathcal{G}_t), t \in \{0, \dots, N-1\}. \end{aligned}$$

Theorem 1 *If \mathbf{u}^* is optimal for Problem 1, 2, or 3, then \mathbf{u}^* is optimal for the remaining two problems.*

Proof. We already explained the above statement regarding Problems 1 and 2 in Section 3. Now, since the objectives of Problems 2 and 3 are identical, it suffices to confirm that their constraints are equivalent. We showed that the original dynamics (1) can be lifted to the augmented dynamics (11) previously in Section 4. Conversely, (11) can be reduced to (1) by considering the first n entries of η_{t+1} . Problems 2 and 3 have the same initial condition $\eta_0 = x_0 = \mathbf{x}_0$ a.s. To see that their control constraints are equivalent, first observe that $g_t = h_t$ if $\mathbf{k} = 0$. Otherwise, if $\mathbf{k} \geq 1$, then g_t and h_t are still measurable maps of each other, leading to $u_t \in \mathcal{L}^2(\mathcal{F}_t)$ if and only if $u_t \in \mathcal{L}^2(\mathcal{G}_t)$. \square

Overall, we have reformulated the original nonstandard problem (Problem 1) into a problem (Problem 3) that enjoys a standard form, and more specifically, a standard dynamic-programming-based solution.

Corollary 1 *Let all conditions and definitions pertaining to Problem 3 hold. Define the functions J_t on \mathbb{R}^{n_t} by $J_N := c_N$, and for each $t = N-1, \dots, 0$,*

$$J_t(\eta) := \inf_{u \in \mathbb{R}^m} \left(c_t(\eta, u) + \mathbb{E}(J_{t+1}(f_t(\eta, u, w_t))) \right). \quad (12)$$

Then, J_t is convex quadratic for every $t \in \{0, \dots, N\}$ and an affine function $\mu_t^ : \mathbb{R}^{n_t} \rightarrow \mathbb{R}^m$ attains the infimum in (12) for every $t \in \{0, \dots, N-1\}$. In addition,*

$\mathbf{u}^* := (u_0^*, \dots, u_{N-1}^*)$, where $u_t^* := \mu_t^* \circ \eta_t$, is an optimal controller for Problem 3, and the optimal value of Problem 3 is $J_\lambda^*(\mathbf{x}_0) = J_0(\mathbf{x}_0)$. Particularly, for every $t \in \{0, \dots, N-1\}$ and $\eta \in \mathbb{R}^{n_t}$, we have

$$J_t(\eta) = \eta^\top P_t \eta + q_t^\top \eta + r_t \quad \text{and} \quad \mu_t^*(\eta) = K_t \eta + \kappa_t,$$

where $P_t \in \mathcal{S}_{n_t}$, q_t , r_t , K_t , and κ_t satisfy the following Riccati recursion:

$$\begin{aligned} P_t &:= -\tilde{A}_t^\top P_{t+1} \tilde{B}_t (\tilde{B}_t^\top P_{t+1} \tilde{B}_t + R)^{-1} \tilde{B}_t^\top P_{t+1} \tilde{A}_t \\ &\quad + \mathcal{Q}_{\lambda,t} + \tilde{A}_t^\top P_{t+1} \tilde{A}_t \\ q_t &:= \lambda \zeta_t + (\tilde{A}_t + \tilde{B}_t K_t)^\top (q_{t+1} + 2P_{t+1} \tilde{C}_t \bar{w}) \\ r_t &:= r_{t+1} + \text{tr}((\Sigma + \bar{w} \bar{w}^\top) \tilde{C}_t^\top P_{t+1} \tilde{C}_t) + q_{t+1}^\top \tilde{C}_t \bar{w} \\ &\quad - \kappa_t^\top (\tilde{B}_t^\top P_{t+1} \tilde{B}_t + R) \kappa_t \\ K_t &:= -(\tilde{B}_t^\top P_{t+1} \tilde{B}_t + R)^{-1} \tilde{B}_t^\top P_{t+1} \tilde{A}_t \\ \kappa_t &:= -\frac{1}{2} (\tilde{B}_t^\top P_{t+1} \tilde{B}_t + R)^{-1} \tilde{B}_t^\top (q_{t+1} + 2P_{t+1} \tilde{C}_t \bar{w}) \end{aligned}$$

with $P_N := \mathcal{Q}_{\lambda,N}$, $q_N := \lambda \zeta_N$, and $r_N := 0$.

Proof. The result follows from dynamic programming, e.g., see [21, Th. 3.2.1] and [28, Ch. 6, Th. 2.15], where the model is nonstationary [21, p. 32] because the state space \mathbb{R}^{n_t} , the dynamics map f_t , and the stage cost function c_t depend on time. The optimal values of Problems 2 and 3 are equal (proof of Theorem 1); the optimal value of Problem 3 is $J_0(\mathbf{x}_0)$; and we denoted the optimal value of Problem 2 by $J_\lambda^*(\mathbf{x}_0)$. Hence, $J_\lambda^*(\mathbf{x}_0) = J_0(\mathbf{x}_0)$. \square

Let us comment on the structure of \mathbf{u}^* . First, at each time t , the control u_t^* is an affine feedback of the truncated state history η_t , which contains at most $\mathbf{k}+1$ recent states, instead of the full history. Second, $\tilde{B}_t^\top P_{t+1} \tilde{B}_t + R \in \mathcal{S}_m^+$ is the only matrix being inverted in the recursion, and its dimension does not depend on \mathbf{k} . Third, if $\mathbf{k} = 0$, then \mathbf{u}^* simplifies to the predictive variance controllers (without temporal coupling) in [44, Th. 2] and [43, Th. 5]. If furthermore $\lambda = 0$ and $\bar{w} = 0_{n \times 1}$, then \mathbf{u}^* becomes the linear state-feedback controller for standard stochastic LQR. While enjoying a familiar analytical form, \mathbf{u}^* in the case of $\mathbf{k} \geq 1$ allows the user to consider the aims of state regulation and temporal variability reduction simultaneously, as illustrated next.

5 Numerical Examples

Consider a point mass moving in a two-dimensional μ - ν -plane according to a discrete-time dynamics model $x_{t+1} = Ax_t + Bu_t + B\xi_t$ for $t \in \{0, \dots, N-1\}$, where

$$A = \begin{bmatrix} 1 & T_s & 0 & 0 \\ 0 & 1 & 0 & 0 \\ 0 & 0 & 1 & T_s \\ 0 & 0 & 0 & 1 \end{bmatrix}, \quad B = \begin{bmatrix} 0 & 0 \\ \frac{T_s}{M} & 0 \\ 0 & 0 \\ 0 & \frac{T_s}{M} \end{bmatrix},$$

$T_s = 0.2$ is the sampling period, $M = 1$ is the mass, and $N = 100$. x_t contains position $p_t := [p_{t,\mu} \ p_{t,\nu}]^\top = [x_{t,1} \ x_{t,3}]^\top$ and velocity; $x_{t,2}$ represents velocity in the μ -direction. u_t is the control force, while $\xi_t := [\xi_{t,\mu} \ \xi_{t,\nu}]^\top$ is the disturbance force. As well as ξ_0, \dots, ξ_{N-1} being i.i.d., $\xi_{t,\mu}$ and $\xi_{t,\nu}$ are independent for each t . The point mass occasionally experiences a jolt in the μ -direction, resembling examples from [11, 43, 44], modeled via the distribution of ξ_t . Precisely, $\xi_{t,\mu}$ has a Gaussian mixture distribution $0.8 \times \mathcal{N}(0, 10) + 0.2 \times \mathcal{N}(70, 70)$, whereas $\xi_{t,\nu}$ has a Gaussian distribution $\mathcal{N}(0, 10)$. Hence, $B\xi_t$ satisfies Assumption (A2). For a fixed \mathbf{k} , $\beta \geq 0$, and $Q \in \mathcal{S}_n$, we use an instance of z_t (2) such that $z_t = x_t^\top Q x_t + \beta \sum_{i=1}^{\mathbf{k}} (x_t - x_{t-i})^\top Q (x_t - x_{t-i})$ for $t \geq \mathbf{k}$. We set $\mathbf{x}_0 = [5 \ 0 \ 5 \ 0]^\top$, $R = I_2$, and $Q = \text{diag}(2, 0.1, 1, 0.1)$. Our code is available from https://github.com/AlfredWei1/Temporal_Coupling_2026.

In what follows, we examine the effect of different choices of $\theta := (\beta, \mathbf{k}, \lambda)$ on system performance using metrics that intuitively describe the behavior of the point mass, instead of ones that precisely match the objective (5):

- Total distance traveled $\mathcal{D}_{\text{tot}} := \sum_{t=1}^N |p_t - p_{t-1}|$;
- Total control effort $\mathcal{U}_{\text{tot}} := \sum_{t=0}^{N-1} |u_t|$;
- Max distance from the origin $\mathcal{P}_{\text{max}} := \max_{t=0, \dots, N} |p_t|$;
- Their respective means $\bar{\mathcal{D}}_{\text{tot}}$, $\bar{\mathcal{U}}_{\text{tot}}$, and $\bar{\mathcal{P}}_{\text{max}}$ over some set of simulations;
- Length $\ell_{t,i}$ of the interval centered at the median of $x_{t,i}$ that contains 95% of the samples of $x_{t,i}$ for $i \in \{1, 2\}$.

We quantify temporal variability, control effort, stabilization, and stochastic variability in terms of $\bar{\mathcal{D}}_{\text{tot}}$, $\bar{\mathcal{U}}_{\text{tot}}$, $\bar{\mathcal{P}}_{\text{max}}$, and $(\ell_{t,1}, \ell_{t,2})$ vs. t , respectively. Their relative importance in tuning θ is application-specific, and we leave the choice of an “optimal” θ to the user. We use the notation $\theta = (\beta, \mathbf{k}, \lambda)$ to refer to \mathbf{u}^* with that choice of θ .

First, we depict the behavior of the point mass when $\beta = \mathbf{k} = 1$ for three values of λ in Fig. 1(a). As λ increases, we observe reductions in stochastic and temporal variabilities, along with a rise in control effort. The tradeoff between stochastic variability and control effort is consistent with knowledge about the original predictive variance controller [44, Figs. 3–4]. The case of $\lambda = 1$ (θ_2) offers a middle ground with reduced stochastic variability and some deviation from the origin (see the mean positions near the origin). In contrast, the case of $\lambda = 6$ (θ_3) exhibits more reduction in $\ell_{t,2}$ but also more deviation from the origin.

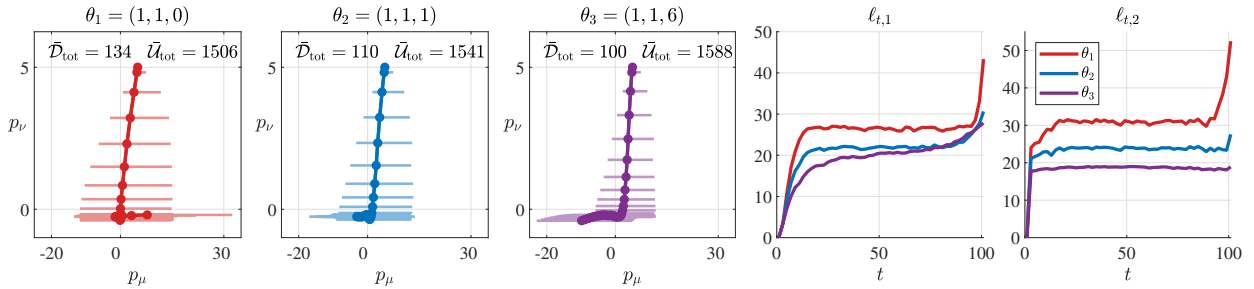
In Fig. 1(b), we consider the controller from [44] (θ_4) and two controllers with temporal coupling (θ_5, θ_6), all with $\lambda = 1$. At the cost of larger control effort, θ_5 and θ_6 lead to smaller temporal variability (see $\bar{\mathcal{D}}_{\text{tot}}$); this is also evident from their more densely spaced mean positions in the early horizon. Thus, temporal coupling enables

the generation of slowly varying trajectories, as anticipated. We also find that temporal coupling can reduce uncertainty. Despite λ being fixed, stochastic variability is typically smaller in the cases of θ_5 and θ_6 compared to θ_4 . Seeing a large increase in $\bar{\mathcal{U}}_{\text{tot}}$ but little change in $\bar{\mathcal{D}}_{\text{tot}}$ in the case of θ_6 versus that of θ_5 , next we study the effect of varying β , \mathbf{k} , and λ simultaneously.

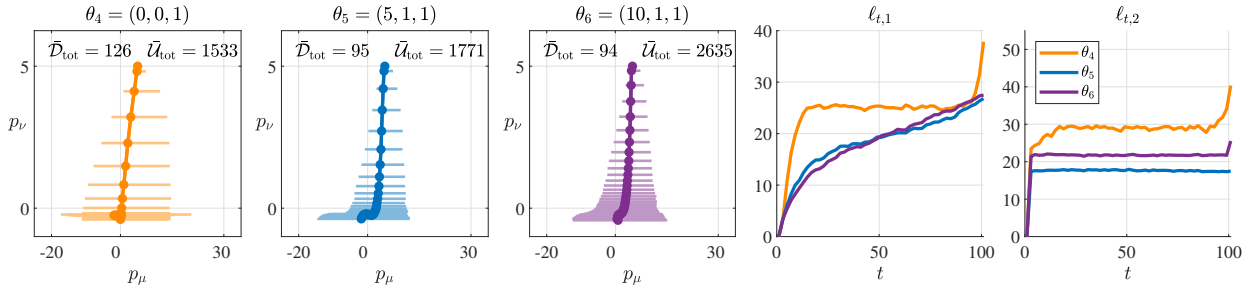
We present $\bar{\mathcal{D}}_{\text{tot}}$ and $\bar{\mathcal{U}}_{\text{tot}}$ versus $\bar{\mathcal{P}}_{\text{max}}$ in Fig. 2 for performance analysis. Fig. 2(i.c) indicates that the choice of $\mathbf{k} = \lambda = 1$ exhibits marginal improvement in $\bar{\mathcal{D}}_{\text{tot}}$ at the cost of accelerating $\bar{\mathcal{U}}_{\text{tot}}$ as β increases. However, for some choices of $\mathbf{k} > 1$ and $\lambda > 0$, the $\bar{\mathcal{U}}_{\text{tot}}$ versus $\bar{\mathcal{P}}_{\text{max}}$ curve does not accelerate as such, but at the price of increasing $\bar{\mathcal{P}}_{\text{max}}$ (Fig. 2(ii.b, iii.b, ii.c, iii.c)). In the case of $\mathbf{k} = 9$ and $\lambda = 0$ (Fig. 2(iii.a)), the $\bar{\mathcal{D}}_{\text{tot}}$ versus $\bar{\mathcal{P}}_{\text{max}}$ curve continues to improve as β increases, but with rising control effort; $\beta = 10$ achieves the lowest values of $\bar{\mathcal{D}}_{\text{tot}}$ and $\bar{\mathcal{P}}_{\text{max}}$ simultaneously across all parameter choices in Fig. 2. Yet, this benefit comes at the cost of larger control effort compared to the choices we investigate next.

We consider $\theta_8 := (2, 9, 0)$ and $\theta_9 := (1.5, 9, 0.2)$, which have approximately the same $\bar{\mathcal{U}}_{\text{tot}}$. Fig. 1(b,c) presents the behavior of the point mass under θ_8, θ_9 , and the benchmarks $\theta_4, \theta_7 := (0, 0, 0)$. Compared to θ_7 , θ_4 reduces stochastic variability (Fig. 1(c)) but exerts more control effort, a known tradeoff [44] (mentioned before). θ_4 also reduces temporal variability compared to θ_7 . Exerting even more control effort, θ_8 and θ_9 further reduce stochastic and temporal variabilities. θ_8 outperforms θ_9 in terms of $\ell_{t,1}$ after about $t = 30$, whereas θ_9 generally outperforms θ_8 in terms of $\ell_{t,2}$. The ability of θ_9 to reduce uncertainty in $x_{t,2}$ is not so surprising due to the specific form of Σ and γ in our setup. Most entries of Σ and γ are zero or small, but Σ_{22} and γ_2 , which correspond to $x_{t,2}$, are large. The superior uncertainty reduction in $x_{t,2}$ under θ_9 comes at the cost of more deviation from the origin, evident from a larger drift in the mean positions, compared to the drift observed under θ_8 .

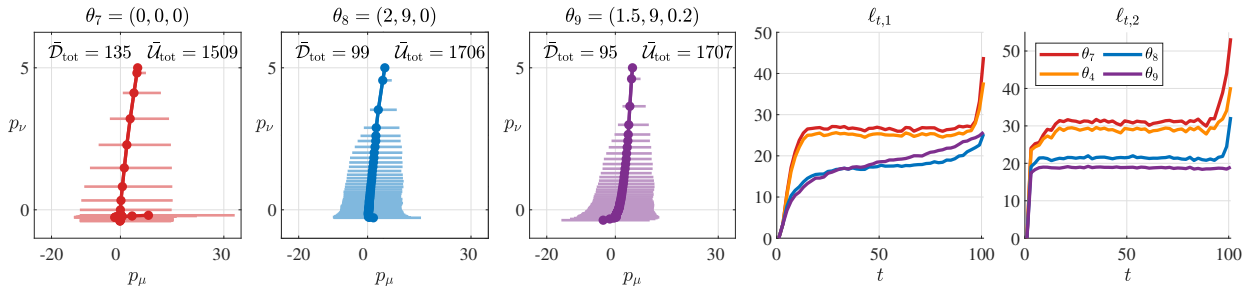
The results herein show various tradeoffs and behaviors that can arise under \mathbf{u}^* with different choices of θ . We experimented with parameter values and used plots of $\bar{\mathcal{D}}_{\text{tot}}$, $\bar{\mathcal{U}}_{\text{tot}}$, and $\bar{\mathcal{P}}_{\text{max}}$ (e.g., see Fig. 2) to select values that led to interpretable trends. The results are specific to the setup and parameter values. For instance, a preliminary experiment revealed that a different choice of (β, \mathbf{k}) than that in Fig. 1(a) did not consistently reduce $\ell_{t,1}$ with increasing λ —a reasonable finding because \mathbf{u}^* (in the case of $\lambda > 0$) is designed to penalize uncertainty in z_t (2), which involves more states than just $x_{t,1}$. To apply \mathbf{u}^* in a different setting, the user may start by generating plots like those in Fig. 2 to inform parameter selection as appropriate for their application.



(a) First experiment for controllers $\theta_1, \theta_2, \theta_3$, with $\beta = \mathbf{k} = 1$ and $\lambda \in \{0, 1, 6\}$.



(b) Second experiment for controllers $\theta_4, \theta_5, \theta_6$, with $\lambda = 1$; θ_4 is from [44]; $(\beta, \mathbf{k}) = (5, 1)$ for θ_5 and $(10, 1)$ for θ_6 .



(c) Third experiment for controllers $\theta_7, \theta_8, \theta_9$; we repeat θ_4 from (b) in the $\ell_{t,1}$ and $\ell_{t,2}$ plots for the sake of comparison.

Fig. 1. Performance of various controllers. Each row compares a set of controllers. Columns 1–3: Trajectories of the point mass from 5000 simulations under \mathbf{u}^* with some choice of $\theta = (\beta, \mathbf{k}, \lambda)$, and the corresponding values of $\bar{\mathcal{D}}_{\text{tot}}$ and $\bar{\mathcal{U}}_{\text{tot}}$; for each $t \in \{0, 2, 4, \dots, 100\}$, we show the associated empirical mean position (dot) and interval of length $\ell_{t,1}$ containing 95% of the samples of $p_{t,\mu}$ (centered at the median of $p_{t,\mu}$). Columns 4–5: $\ell_{t,1}$ and $\ell_{t,2}$ versus t .

6 Conclusion

This work presents a trajectory-wise risk concept that, when incorporated into an optimal control problem for a stochastic linear system, admits an elegant closed-form solution. The derived controller \mathbf{u}^* can be viewed as one that shapes a stochastic state trajectory, penalizing variability of the trajectory over time and also in a probabilistic sense. In the case of $\lambda > 0$, \mathbf{u}^* admits an explicit risk-aware interpretation, while this benefit is lost in the case of $\lambda = 0$. Nonetheless, we found experimentally that \mathbf{u}^* with large \mathbf{k} and $\lambda = 0$ can result in risk-aware system behavior (see θ_8 in Fig. 1(c)). Future research can examine further connections between temporal coupling and risk, possibly in other systems. Temporal or trajectory-wise risk concepts have potential utility in other stochastic control problems, such as those

involving systems with data-based trajectory-wise representations and systems with time delays. We hope the results presented here inspire other notions of risk and associated controllers that can be computed efficiently.

Acknowledgements

M.P.C. thanks Manfredi Maggiore, Laurent Lessard, Marco Pavone, and Anirudha Majumdar for advice.

A Proof of Lemma 1

The proof consists of two main steps. First, we prove the decomposition $\Delta_t^2 = \Delta_{t,1} + \Delta_{t,2} + \Delta_{t,3}$ a.s. (8a). Second, we consider the individual terms in the sum. $\Delta_{t,1}$ was found to be integrable and its expectation was computed

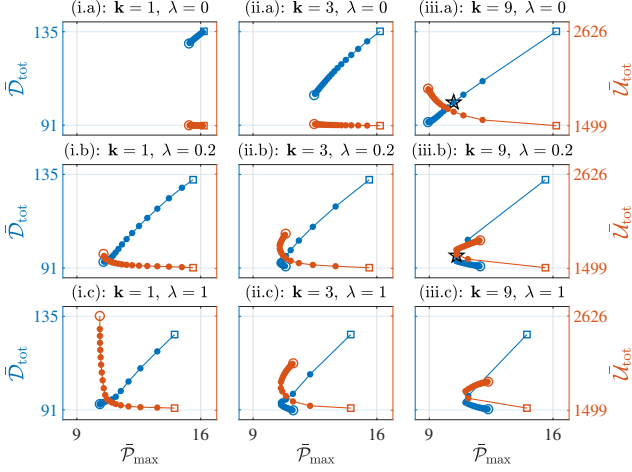


Fig. 2. \bar{D}_{tot} versus \bar{P}_{max} (blue) and \bar{U}_{tot} versus \bar{P}_{max} (red) calculated from 500 simulations for each $\theta = (\beta, \mathbf{k}, \lambda)$. In each subplot, $\beta \in \{0, 0.5, \dots, 10\}$ is varied for each fixed (\mathbf{k}, λ) . The square and circle markers indicate $\beta = 0$ and $\beta = 10$, respectively. Note that $\beta = 0$ represents the absence of temporal coupling, and corresponds to the controller from [44] if $\lambda > 0$. A star marker corresponds to $\theta_8 = (2, 9, 0)$ or $\theta_9 = (1.5, 9, 0.2)$.

using elementary probability theory in [44, Appendix]. We justify why $\Delta_{t,2}$ and $\Delta_{t,3}$ are integrable and compute their expectations using elementary probability theory and any past state x_τ for $\tau \in \{0, \dots, t-1\}$ being \mathcal{F}_{t-1} -measurable. We find the following basic facts useful.

Proposition 1 *Let x and y be \mathbb{R}^n -valued random vectors defined on $(\Omega, \mathcal{G}, \mathbb{P})$, whose expectations exist.*

- (a) *Let \mathcal{F} be a sub- σ -algebra of \mathcal{G} . If y is \mathcal{F} -measurable and $\mathbb{E}(|x_i|), \mathbb{E}(|x_i y_i|) < \infty$ for every $i \in \{1, \dots, n\}$, then $\mathbb{E}(x^\top y | \mathcal{F}) = \mathbb{E}(x | \mathcal{F})^\top y = y^\top \mathbb{E}(x | \mathcal{F})$ a.s.*
- (b) *If x and y are independent and integrable, then $x^\top y$ is integrable and $\mathbb{E}(x^\top y) = \mathbb{E}(x)^\top \mathbb{E}(y)$.*

Proof. (a): The statement follows from [3, Th. 6.5.11(a)]. (b): For any $i \in \{1, \dots, n\}$, x_i and y_i are independent and integrable, so $\mathbb{E}(x_i y_i) = \mathbb{E}(x_i) \mathbb{E}(y_i) \in \mathbb{R}$ [3, Th. 5.10.8]. Since the order of finitely many expectations and sums can be switched when working with integrable random variables [3, Th. 1.6.3], $\mathbb{E}(x^\top y) = \mathbb{E}(\sum_{i=1}^n x_i y_i) = \sum_{i=1}^n \mathbb{E}(x_i y_i) = \sum_{i=1}^n \mathbb{E}(x_i) \mathbb{E}(y_i) = \mathbb{E}(x)^\top \mathbb{E}(y)$. \square

Proposition 2 (From [32, Lemma 4.2]) *Let all random objects to be specified be defined on $(\Omega, \mathcal{G}, \mathbb{P})$. Let $\mathcal{F} = \sigma(h)$, where h is a random vector. Let v and w be \mathcal{F} -measurable, square-integrable, \mathbb{R}^m - and \mathbb{R}^n -valued random vectors, respectively. Let M be an integrable, $\mathbb{R}^{m \times n}$ -valued random matrix independent of h . Then, $v^\top M w$ is integrable and $\mathbb{E}(v^\top M w | \mathcal{F}) = v^\top \mathbb{E}(M) w$ a.s.*

We now proceed to proving Lemma 1.

Step 1) First, consider the case of $\mathbf{k}_t \geq 1$. Define $\hat{x}_t := \mathbb{E}(x_t | \mathcal{F}_{t-1}) = Ax_{t-1} + Bu_{t-1} + \bar{w}$ a.s., which is \mathcal{F}_{t-1} -measurable. Since x_0, \dots, x_N are square-integrable random vectors under Assumption 1, all terms in the expansion (6) of z_t are integrable random variables. Then,

$$\mathbb{E}(z_t | \mathcal{F}_{t-1}) \stackrel{\text{a.s.}}{=} \sum_{i=1}^{\mathbf{k}_t} \sum_{j=1}^{\mathbf{k}_t} x_{t-i}^\top Q_{ij} x_{t-j} + 2 \sum_{i=1}^{\mathbf{k}_t} x_{t-i}^\top Q_{i0} \hat{x}_t + \mathbb{E}(x_t^\top Q_{00} x_t | \mathcal{F}_{t-1})$$

in particular by linearity of conditional expectation [3, Th. 6.5.2(a)] and Proposition 1(a) with x_{t-i} being \mathcal{F}_{t-1} -measurable for every $i \in \{1, \dots, \mathbf{k}_t\}$. Using $x_t - \hat{x}_t = d_t$ a.s., we can compute Δ_t from its definition to find that $\Delta_t = 2 \sum_{i=1}^{\mathbf{k}_t} x_{t-i}^\top Q_{i0} d_t + y_t$ a.s., and squaring this expression for Δ_t gives (8a). Now, in the case of $\mathbf{k}_t = 0$, we have $z_t = x_t^\top Q_{00} x_t$, leading to $\Delta_t = y_t$.

Step 2a) Computation of $\mathbb{E}(\Delta_{t,2})$. For each i and j in $\{1, \dots, \mathbf{k}_t\}$, the random vectors x_{t-i} and x_{t-j} are \mathcal{F}_{t-1} -measurable and square-integrable, and the random matrix $Q_{i0} d_t d_t^\top Q_{0j}$ is integrable and independent of h_{t-1} . Hence, by Proposition 2, $x_{t-i}^\top Q_{i0} d_t d_t^\top Q_{0j} x_{t-j}$ is integrable and $\mathbb{E}(x_{t-i}^\top Q_{i0} d_t d_t^\top Q_{0j} x_{t-j} | \mathcal{F}_{t-1}) = x_{t-i}^\top Q_{i0} \Sigma Q_{0j} x_{t-j}$ a.s. Taking the expectation, applying the law of total expectation, and summing over i and j leads to (8c).

Step 2b) Computation of $\mathbb{E}(\Delta_{t,3})$. It can be shown [44, Appendix] that

$$y_t = d_t^\top Q_{00} d_t - \text{tr}(\Sigma Q_{00}) + 2\hat{x}_t^\top Q_{00} d_t \quad \text{a.s.} \quad (\text{A.1})$$

We substitute (A.1) into (7c) to obtain $\Delta_{t,3} = 4 \sum_{i=1}^{\mathbf{k}_t} \alpha_{1i} + \alpha_{2i} + \alpha_{3i}$ a.s., where

$$\begin{aligned} \alpha_{1i} &:= x_{t-i}^\top Q_{i0} d_t d_t^\top Q_{00} d_t, \\ \alpha_{2i} &:= -x_{t-i}^\top Q_{i0} d_t \text{tr}(\Sigma Q_{00}), \quad \text{and} \\ \alpha_{3i} &:= 2x_{t-i}^\top Q_{i0} d_t d_t^\top Q_{00} \hat{x}_t. \end{aligned}$$

Every α_{1i} and α_{2i} are integrable by Proposition 1(b), and every α_{3i} is integrable by Proposition 2. Thus, $\Delta_{t,3}$ is also integrable. Computing their expectations $\mathbb{E}(\alpha_{1i}) = \mathbb{E}(x_{t-i}^\top Q_{i0} \gamma)$, $\mathbb{E}(\alpha_{2i}) = 0$, and $\mathbb{E}(\alpha_{3i}) = 2\mathbb{E}(x_{t-i}^\top Q_{i0} \Sigma Q_{00} x_t)$ leads to (8d). More details follow. To compute $\mathbb{E}(\alpha_{1i})$ and $\mathbb{E}(\alpha_{2i})$, one can apply Proposition 1(b), particularly using the properties that x_{t-i} is integrable and \mathcal{F}_{t-1} -measurable, w_{t-1} and h_{t-1} are independent, $\mathbb{E}(d_t d_t^\top Q_{00} d_t) = \gamma \in \mathbb{R}^n$, and $\mathbb{E}(d_t) = 0_{n \times 1}$. To compute $\mathbb{E}(\alpha_{3i})$, first one can apply Proposition 2, $\mathbb{E}(d_t d_t^\top) = \Sigma \in \mathbb{R}^{n \times n}$, and the law of total expectation to derive $\mathbb{E}(\alpha_{3i}) = \mathbb{E}(2x_{t-i}^\top Q_{i0} \Sigma Q_{00} \hat{x}_t)$. Observe that $x_{t-i}^\top Q_{i0} \Sigma Q_{00} x_t$ is integrable because x_{t-i}

and x_t are square-integrable. Hence, it follows from the law of total expectation and Proposition 1(a) that

$$\begin{aligned}\mathbb{E}(x_{t-i}^\top Q_{i0} \Sigma Q_{00} x_t) &= \mathbb{E}(\mathbb{E}(x_{t-i}^\top Q_{i0} \Sigma Q_{00} x_t | \mathcal{F}_{t-1})) \\ &= \mathbb{E}(x_{t-i}^\top Q_{i0} \Sigma Q_{00} \mathbb{E}(x_t | \mathcal{F}_{t-1})) \\ &= \mathbb{E}(x_{t-i}^\top Q_{i0} \Sigma Q_{00} \hat{x}_t),\end{aligned}$$

which completes the proof. \square

References

- [1] P. Akella, A. Dixit, M. Ahmadi, L. Lindemann, M. P. Chapman, G. J. Pappas, A. D. Ames, and J. W. Burdick. Risk-aware robotics: Tail risk measures in planning, control, and verification [Focus on education]. *IEEE Control Syst.*, 45(4):46–78, 2025.
- [2] A. Artuñedo, J. Villagra, and J. Godoy. Jerk-limited time-optimal speed planning for arbitrary paths. *IEEE Trans. Intell. Transp. Syst.*, 23(7):8194–8208, 2021.
- [3] R. B. Ash. *Real Analysis and Probability*. Academic Press, Inc., New York, NY, USA, 1972.
- [4] F. Bacchus, C. Boutilier, and A. Grove. Rewarding behaviors. In *Proc. 13th Nat. Conf. Artif. Intell.*, pages 1160–1167, 1996.
- [5] N. Bäuerle and A. Glauner. Markov decision processes with recursive risk measures. *Eur. J. Oper. Res.*, 296(3):953–966, 2022.
- [6] N. Bäuerle and J. Ott. Markov decision processes with average-value-at-risk criteria. *Math. Meth. Oper. Res.*, 74(3):361–379, 2011.
- [7] N. Bäuerle and U. Rieder. More risk-sensitive Markov decision processes. *Math. Oper. Res.*, 39(1):105–120, 2014.
- [8] A. Biswas and V. S. Borkar. Ergodic risk-sensitive control—A survey. *Annu. Rev. Control*, 55:118–141, 2023.
- [9] M. P. Chapman, R. Bonalli, K. M. Smith, I. Yang, M. Pavone, and C. J. Tomlin. Risk-sensitive safety analysis using conditional value-at-risk. *IEEE Trans. Autom. Control*, 67(12):6521–6536, 2022.
- [10] M. P. Chapman, M. Fauß, and K. M. Smith. On optimizing the conditional value-at-risk of a maximum cost for risk-averse safety analysis. *IEEE Trans. Autom. Control*, 68(6):3720–3727, 2023.
- [11] M. P. Chapman and D. Kalogerias. Risk-aware stability of linear systems. *IEEE Trans. Autom. Control*, 70(2):861–876, 2025.
- [12] R. Chen, Y. Li, and T. Chai. Risk-constrained MPC with application in safety-critical control of turbofan engines. *IEEE Trans. Automat. Sci. Eng.*, 22:872–882, 2025.
- [13] L. Consolini and M. Locatelli. Is time-optimal speed planning under jerk constraints a convex problem? *Automatica*, 169:111864, 2024.
- [14] X.-Y. Cui, J.-J. Gao, X. Li, and Y. Shi. Survey on multi-period mean–variance portfolio selection model. *J. Operations Res. Soc. China*, 10(3):599–622, 2022.
- [15] A. Del Prete. Joint position and velocity bounds in discrete-time acceleration/torque control of robot manipulators. *IEEE Robot. Automat. Lett.*, 3(1):281–288, 2017.
- [16] A. Dixit, D. D. Fan, K. Otsu, S. Dey, A.-A. Agha-Mohammadi, and J. Burdick. STEP: Stochastic traversability evaluation and planning for risk-aware navigation; results from the DARPA subterranean challenge. *Field Robot.*, 4:182–210, 2024.
- [17] K. Fujimoto, S. Ogawa, Y. Ota, and M. Nakayama. Optimal control of linear systems with stochastic parameters for variance suppression: The finite time horizon case. In *18th IFAC World Congress*, pages 12605–12610. IFAC, 2011.
- [18] K. Glover and J. C. Doyle. State-space formulae for all stabilizing controllers that satisfy an H_∞ -norm bound and relations to risk sensitivity. *Syst. Control Lett.*, 11(3):167–172, 1988.
- [19] C. Guarino Lo Bianco and F. Ghilardelli. A discrete-time filter for the generation of signals with asymmetric and variable bounds on velocity, acceleration, and jerk. *IEEE Trans. Ind. Electron.*, 61(8):4115–4125, 2014.
- [20] C. Guarino Lo Bianco, A. Tonielli, and R. Zanasi. Nonlinear trajectory generator for motion control systems. In *Proc. 1996 IEEE IECON. 22nd Int. Conf. Ind. Electron., Control, and Instrum.*, volume 1, pages 195–201.
- [21] O. Hernández-Lerma and J. B. Lasserre. *Discrete-Time Markov Processes: Basic Optimality Criteria*. Springer-Verlag, New York, NY, USA, 1996.
- [22] R. A. Horn and C. R. Johnson. *Matrix Analysis*. Cambridge Univ. Press, New York, NY, USA, 2nd edition, 2013.
- [23] D. A. Iancu, M. Petrik, and D. Subramanian. Tight approximations of dynamic risk measures. *Math. Operations Res.*, 40(3):655–682, 2015.
- [24] H. Jia and Y.-H. Ni. Decentralized stochastic linear-quadratic optimal control with risk constraint and partial observation. *Syst. Control Lett.*, 187:105778, 2024.
- [25] M. Jones and M. M. Peet. Extensions of the dynamic programming framework: Battery scheduling, demand charges, and renewable integration. *IEEE Trans. Autom. Control*, 66(4):1602–1617, 2020.
- [26] B. Kang, C. Aduba, and C.-H. Won. Statistical control for performance shaping using cost cumulants. *IEEE Trans. Autom. Control*, 59(1):249–255, 2014.
- [27] M. Kishida and A. Cetinkaya. Risk-aware linear quadratic control using conditional value-at-risk. *IEEE Trans. Autom. Control*, 68(1):416–423, 2022.
- [28] P. R. Kumar and P. Varaiya. *Stochastic Systems: Estimation, Identification, and Adaptive Control*. Prentice-Hall, Inc., Englewood Cliffs, NJ, USA, 1986.
- [29] A. Majumdar and M. Pavone. How should a robot assess risk? Towards an axiomatic theory of risk in robotics. In N. Amato, G. Hager, S. Thomas, and M. Torres-Torriti, editors, *Robotics Research. Springer Proceedings in Advanced Robotics*, volume 10, pages 75–84, Cham, Switzerland, 2020.
- [30] F. Oldewurtel, C. N. Jones, A. Parisio, and M. Morari. Stochastic model predictive control for building climate control. *IEEE Trans. Control Syst. Technol.*, 22(3):1198–1205, 2013.
- [31] E. Papachristoforou, V. Lambadiari, E. Maratou, and K. Makrilakis. Association of glycemic indices (hyperglycemia, glucose variability, and hypoglycemia) with oxidative stress and diabetic complications. *J. Diabetes Res.*, 2020(1):7489795, 2020.
- [32] D. Patel. Risk-aware control of cone-bounded nonlinear systems. MASc thesis, Edward S. Rogers Sr. Dept. Elect. Comput. Eng., Univ. Toronto, Toronto, ON, Canada, 2025.
- [33] D. Patel and M. P. Chapman. Risk-aware control of systems with quasi-cone-bounded nonlinearities. To be submitted to or already under review for *Automatica*.
- [34] D. Patel and M. P. Chapman. Risk-aware finite-horizon social optimal control of mean-field coupled linear-quadratic subsystems. *IEEE Control Syst. Lett.*, 8:2265–2270, 2024.

- [35] J. O. Royset. Risk-adaptive approaches to stochastic optimization: A survey. *SIAM Rev.*, 67(1):3–70, 2025.
- [36] A. Ruszczyński. Risk-averse dynamic programming for Markov decision processes. *Math. Program.*, 125(2):235–261, 2010.
- [37] M. K. Sain. Control of linear systems according to the minimal variance criterion—A new approach to the disturbance problem. *IEEE Trans. Autom. Control*, 11(1):118–122, 1966.
- [38] M. K. Sain, C.-H. Won, and B. F. Spencer. Cumulants in risk-sensitive control: The full-state-feedback cost variance case. In *1995 34th IEEE Conf. Decis. Control (CDC)*, pages 1036–1041, 1995.
- [39] S. Samuelson and I. Yang. Safety-aware optimal control of stochastic systems using conditional value-at-risk. In *2018 Annu. Amer. Control Conf. (ACC)*, pages 6285–6290. IEEE.
- [40] A. Shapiro, D. Dentcheva, and A. Ruszczyński. *Lectures on Stochastic Programming: Modeling and Theory*. SIAM-MPS, Philadelphia, PA, USA, 2009.
- [41] K. M. Smith and M. P. Chapman. On exponential utility and conditional value-at-risk as risk-averse performance criteria. *IEEE Trans. Control Syst. Technol.*, 31(6):2555–2570, 2023.
- [42] J. Somasundaram, I. Koch, and N. Lim. Raising the AC temperature in the tropics, one degree at a time. *Energy Economics*, 128:107191, 2023.
- [43] A. Tsiamis, D. Kalogieras, A. Ribeiro, and G. J. Pappas. Linear quadratic control with risk constraints. *Automatica*, 174:112095, 2025.
- [44] A. Tsiamis, D. S. Kalogieras, L. F. O. Chamon, A. Ribeiro, and G. J. Pappas. Risk-constrained linear-quadratic regulators. In *2020 59th IEEE Conf. Decis. Control (CDC)*, pages 3040–3047.
- [45] B. P. G. van Parys, D. Kuhn, P. J. Goulart, and M. Morari. Distributionally robust control of constrained stochastic systems. *IEEE Trans. Autom. Control*, 61(2):430–442, 2015.
- [46] Y. Wang and M. P. Chapman. Risk-averse autonomous systems: A brief history and recent developments from the perspective of optimal control. *Artif. Intell.*, 311:103743, 2022.
- [47] Y. Wang, W. Wang, K. Zhang, Y. Xu, and R. Su. Risk-constrained linear quadratic control with one-step delayed sharing information pattern. *Automatica*, 174:112093, 2025.
- [48] P. Whittle. Risk-sensitive linear/quadratic/Gaussian control. *Adv. Appl. Probability*, 13(4):764–777, 1981.
- [49] K. Zhang, B. Hu, and T. Başar. Policy optimization for \mathcal{H}_2 linear control with \mathcal{H}_∞ robustness guarantee: Implicit regularization and global convergence. *SIAM J. Control Optim.*, 59(6):4081–4109, 2021.
- [50] F. Zhao, K. You, and T. Başar. Infinite-horizon risk-constrained linear quadratic regulator with average cost. In *2021 60th IEEE Conf. Decis. Control (CDC)*, pages 390–395.